“Multimode Vibration Cutting” – A New Vibration Cutting for Highly-efficient and Highly-flexible Surface Texturing

Hongjin Jung*[1], Takehiro Hayasaka[1], Eiji Shamoto[1],
Hiroaki Ishii[2], Takashi Ueyama[2], and Seiji Hamada[2]
*hj_jung@nagoya-u.jp
1. Graduate School of Engineering, Nagoya University, Japan
2. Product Development Department, Taga Electric Co. Ltd. Japan

Abstract: This paper proposes a new vibration cutting method named “multimode vibration cutting” for precision surface texturing. The proposed cutting method utilizes multiple unidirectional vibration modes mainly in the depth-of-cut direction. The vibrations at multiple frequencies induced to the tool tip can generate not only sinusoidal but also highly-flexible trajectories such as trapezoidal, triangular, and distorted triangular waves. Notably, only a sinusoidal vibration can be induced when a single resonant vibration is applied to the tool tip. Compared to conventional highly-flexible cutting methods for surface texturing, such as the utilization of fast tool servo and amplitude control of ultrasonic elliptical vibration cutting, the proposed method is highly-efficient because of its direct usage of high resonant frequencies. Compared to conventional highly-efficient cutting methods for surface texturing, such as linear and elliptical vibration cutting which mainly utilizes the vibration component in the depth-of-cut direction, the proposed method can generate highly-flexible trajectories for various micro texture profiles. In this study, an ultrasonic multimode vibration device is developed, and the mechanics of generating multimode vibrations are demonstrated. Turning experiments with several texture profiles are performed to confirm the validity of the proposed method for highly-efficient and highly-flexible micro/nano surface texturing.

Keywords: Cutting, Vibration-assisted cutting, Surface texturing, Multimode vibration cutting

1. Introduction

To endow functional properties to products, micro/nanostructures with appropriate precise patterns can be sculptured on their surfaces. Several studies have demonstrated that textured surfaces can enhance specific characteristics [1] such as hydrophobicity [2], optical functionality [3], and tribological performance [4,5].

Highly-efficient and highly-flexible fabrication technologies are required to practically expand the use of surface texturing. There are several optical and electronic fabrication methods such as laser machining [6, 7], photolithography [8], and electro-chemical machining [9]. However, these methods require long fabrication periods for large surface areas and have restricted machinable materials [10]. Ultraprecision diamond cutting is a prominent micro/nanostructure fabrication method. It is a practical method that allows a high structural degree of freedom and also generates the most accurate and repeatable geometries and the finest surface finishing method among the various machining methods [10, 11]. Moreover, the cutting edges of diamond tools can be manufactured precisely with nanoscale structures to realize high value-added surface texturing [12].

Several studies have been reported about highly-flexible cutting for fabrication of micro/nanostructures. FTS (Fast tool servo)-based diamond machining has been developed for efficient surface texturing [13,14]. To realize precision micro/nano machining of difficult-to-cut materials such as hardened die steel [15,16] and tungsten carbide [17], ultrasonic elliptical vibration cutting with amplitude control has been developed. The rapid tool wear and defects on the finished surface are reduced with this method. However, the efficiencies of these cutting methods are limited by the low bandwidth of the vibration controller which is around 3 kHz [18] for FTS and 300 Hz [15] for amplitude control of elliptical vibration cutting.

To realize highly-efficient surface texturing, ultrasonic vibration of a resonant vibrator has been utilized. Kumabe [19] is thought to be the first to invent this kind of method where the vibration in the depth-of-cut direction is utilized with its amplitude larger than the depth of cut to break up continuous chips and obtain qualified surface roughness. Guo et al. [20] added the vibration in the cutting direction on to Kumabe’s method. The trajectory of the elliptical vibration is transferred to the cut surfaces as a micro/nano structure. However, as the vibration speed is much smaller than the nominal cutting speed in highly-efficient texturing, the vibration in the cutting direction does not have an important meaning. Therefore, it is similar to Kumabe’s method. Xu et al. [21] combined the tool rotation and the ultrasonic vibrations. However, only sinusoidal or distorted sine waves or parts of those waves could be generated by these highly-efficient texturing methods because a single frequency resonant vibration is applied.

In summary, it can be said that there is no precision surface texturing technology which realizes high efficiency and high flexibility simultaneously. In this study, “multimode vibration cutting” is proposed for highly-efficient and highly-flexible micro/nano surface texturing. The proposed technology utilizes multiple unidirectional ultrasonic vibrations in the depth-of-cut direction. By utilizing this method, it is possible to generate sinusoidal as well as sophisticated trajectories at ultrasonic frequencies to realize highly-efficient and highly-flexible texturing, which are impossible to accomplish using conventional technologies.

Several methods related to the combination of different two or more frequencies for precision machining have been developed in the literature. Zhang et al. [22] propose a passive method for surface generations that utilizes the vibrations caused by the cutting forces. Hence, the fabricated structures would be depended on the cutting process, e.g., cutting conditions and tool wear. Other studies [23, 24] have proposed combining the ultrasonic elliptical vibration cutting and FTS to create freeform surfaces on hardened steel. However, although it appears that two different modes are used in the manufacture of freeform surfaces, these vibrations are only vibrating separately in different ranges for two different purposes. For instance, the ultrasonic elliptical vibration is oscillated only for reducing the diamond tool wear. FTS vibration oscillates only for the freeform surface. The efficiency for the fabrication of micro/nanostructures is limited by the low band of FTS, as mentioned above. However, in the proposed method, two or more modes are used directly for the surface texturing, and these vibrations are excited in a specially designed vibration tool. These are the novelties of this study, which are regarded as different from the previous studies.

The basic principle of the multimode vibration cutting is described in Chapter 2. The developed ultrasonic multi-mode vibrator and its dynamic characteristics are explained in Chapter 3. The identification of the cutting and vibration parameters for the cutting of specific target profiles are described in Chapter 4. Face turning experiments for highly-efficient and highly-flexible micro/nano surface texturing with the proposed cutting method and their experimental results are described in Chapter 5. The paper concludes with a summary in Chapter 6.

2. Multimode vibration cutting

Figure 1 shows a schematic of the proposed multimode vibration cutting method. The tool is fed at a nominal cutting speed, and a multimode vibration is applied to the cutting edge in the depth-of-cut direction during the cutting. The multimode vibration here refers to the sum of a plurality of unidirectional vibrations. When each mode frequency is an integer multiple of a standard frequency, the combined vibration becomes periodic without beats. In general, when vibrations with different frequencies are combined, the combined multimode vibration will repeat at a greatest common divisor frequency. For example, if two vibrations, which have the frequencies of 6 kHz (three times 2 kHz) and 10 kHz (five times 2 kHz), are combined, the multimode vibration will repeat at the frequency of 2 kHz.

The multimode vibration is inspired by the Fourier series whereby every periodic vibration can be expressed as a summation of harmonically related sine waves. In this study, the 1st mode vibration (1st half wavelength resonant mode of axial vibration of vibrator) and the vibration corresponding to three times this frequency (3rd resonant mode of axial vibration of vibrator) are used. Since a resonant vibration device and ultrasonic vibration are utilized, highly-efficient surface texturing can be achieved. In addition, the amplitudes and the phase difference of the two modes can be controlled to achieve highly-flexible surface texturing; the two demands of texturing can be accomplished.

Ultrasonic vibrations with trapezoidal, triangular, and distorted triangular waves are generated and tested with the developed vibrator. The vibrator should be designed and built carefully to match the 3rd resonant frequency to three times the 1st resonant frequency as closely as possible to obtain precise multimode vibration with minimal electric power. The locus of the cutting edge, that is, the sum of the nominal cutting velocity and the ultrasonic multimode vibration, is transferred to the textured surface. Furthermore, it is also possible to transfer a part of the locus to the textured surface by adjusting the nominal depth of cut smaller than the amplitudes of the multimode vibration ($d < A_1 + A_3$).

As shown in Fig. 1, there are three categories of adjustable parameters: cutting parameters (d and V_c in the simple two dimensional cutting), tool geometry parameters, and vibration parameters (f_1, f_3, A_1, A_3, and ϕ in the simple case of two frequencies). Here, d and V_c are the nominal depth of cut and nominal cutting velocity, respectively, f_1 and f_3 are the frequencies of the first and third modes, respectively, A_1 and A_3 are their respective amplitudes, and ϕ is the phase difference between the vibrations of the two modes. In this fundamental study of the newly proposed vibration-assisted cutting method, only the cutting parameters and the vibration parameters are considered.

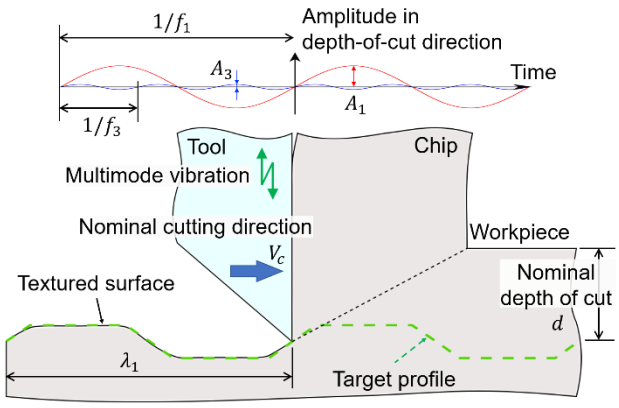

Fig. 1 Surface texturing by ultrasonic multimode vibration cutting.

3. Development and analysis of ultrasonic multimode vibration-cutting device

Figure 2 shows a schematic illustration of the ultrasonic multimode vibration cutting device developed in this work. To generate the multimode vibration, a combined voltage from the sum of one sine wave with a frequency of f_1 and a second sine wave with a frequency of $f_3 = 3f_1$ should be generated by the oscillator. The combined voltage is applied to a piezoelectric actuator through an amplifier. As mentioned above, f_1 and f_3 are identical to the frequencies of the first and third resonant modes of the axial vibration in the depth-of-cut direction. The resonant modes are determined by the structure of the rod-shaped cutting device.

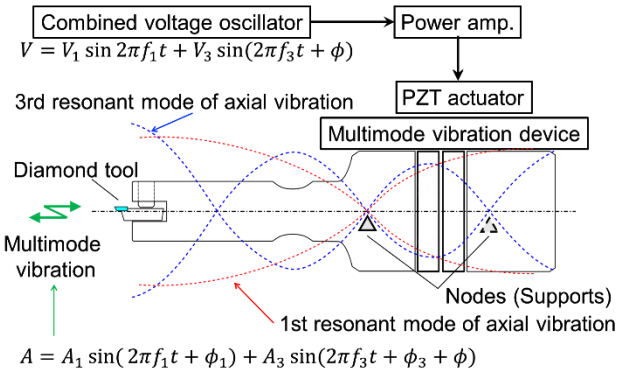

Fig. 2 Driving system of ultrasonic multimode vibration-cutting device.

Figures 3(a) and (b) show the finite element analysis results for the first and third resonant modes of the device. The device resonates at approximately 19 kHz and 57 kHz. The challenges in the device design are as follows. To effectively induce powerful multimode vibrations with a reasonable amount of electrical power, the frequency of the third mode should be close to triple the frequency of the first mode. Then, the nodal positions should be identified and fixed with rigid supports perpendicular to the cutting direction so that the vibrations are generated precisely and efficiently without useless friction for utilization in the cutting device.

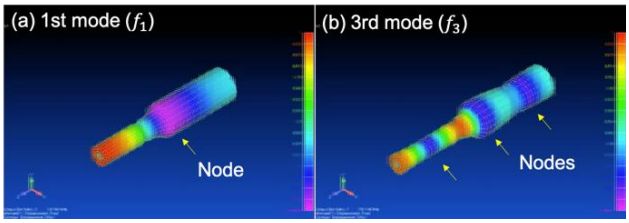

Fig. 3 Results of finite element analysis for ultrasonic multimode vibration device: (a) first half wavelength resonant mode of axial vibration, (b) third resonant mode of axial vibration.

It is necessary to investigate the electrical and mechanical properties of the vibration device in order to precisely induce ultrasonic multimode vibrations. The admittance and transfer function between the applied voltages and excited vibrations are measured in the range of 17.5 kHz to 60 kHz. Figure 4 shows the measurement setup. The developed device is mounted on the table of a precision machine tool (Fujikoshi, NANO ASPHER ASP01UPX). The input voltage V_{in} is generated by a function generator (NF Corporation, WF1974) and amplifier. The output displacement A_{out} of the tool and current i_{out} are measured by a laser Doppler vibrometer (Graphtec Corp., AT3700-AT0042) and an ammeter, respectively. These signals are recorded on a digital oscilloscope, and the admittance and transfer function are calculated on a computer.

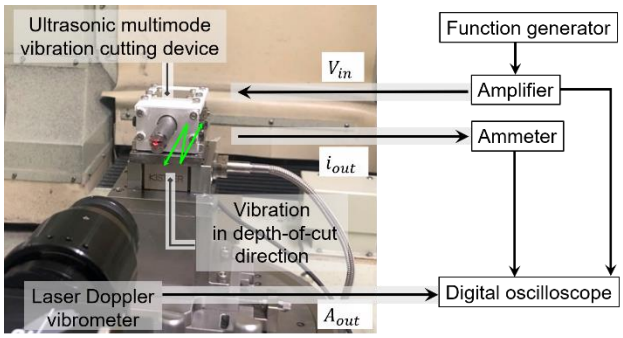

Fig. 4 Experimental setup for measuring mechanical and electrical properties of ultrasonic multimode vibration device.

The admittance Y and transfer function G are derived using the following equations, and the gains and phases are plotted against the input frequency as shown in Fig. 5. Figures 5(a) and (b) show Y and G, respectively.

$$\mathrm{Y}(s) = i_{out}(s)/V_{in}(s), \tag{1}$$
$$\mathrm{G}(s) = A_{out}(s)/V_{in}(s). \tag{2}$$

From the results of the admittance, f_1 is determined as the frequency with the smallest admittance, i.e. antiresonance, and f_3 is determined as three times f_1. Therefore, $f_1 = 19.35$ kHz and $f_3 = 58.05$ kHz. By selecting f_1 as the antiresonance, the vibrations can be induced efficiently with the smallest current. Generally, a change in temperature of the device results in a change in the admittance and transfer function of it. For example, as the temperature increases, the volume of the device increases and the resonant frequency decreases. Hence, these measurements are performed in a temperature-controlled room. Next, the gains G_1 and G_3 and phases ϕ_1 and ϕ_3 are determined from the measured transfer function at the frequencies f_1 and f_3, respectively. Therefore, when a combined voltage is applied to the developed device as represented by Eq. (3), a multimode vibration is induced, as shown in Eq. (4).

$$\mathrm{V} = V_1 \sin 2\pi f_1 t + V_3 \sin(2\pi f_3 t + \phi), \tag{3}$$
$$\begin{aligned}\mathrm{A} &= G_1 V_1 \sin(2\pi f_1 t + \phi_1) \\ &\quad + G_3 V_3 \sin(2\pi f_3 t + \phi_3 + \phi) \\ &= A_1 \sin(2\pi f_1 t + \phi_1) + A_3 \sin(2\pi f_3 t + \phi_3 + \phi)\end{aligned} \tag{4}$$

Here, ϕ is the phase difference between the first and third modes.

The transfer characteristic of each mode is independent and does not affect each other. This is because the induced modes are sufficiently separated from each other in the frequency domain, i.e., they are decoupled. The inverse transfer function is also valid, and the oscillation voltage profile to induce the multimode vibration and to fabricate designed texture surfaces can be determined. This process is described in Chapter 4.

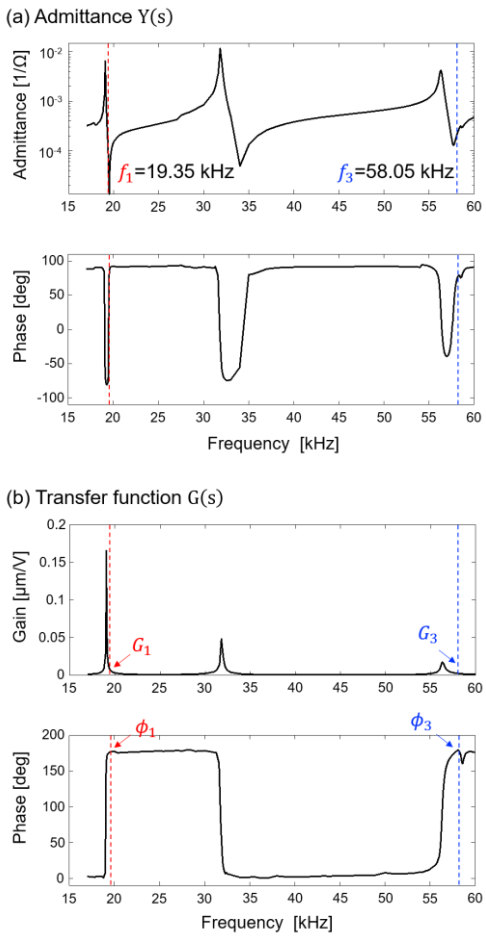

Fig. 5 Measured admittance and transfer function of ultrasonic multimode vibration device: (a) Admittance, (b) Transfer function.

4. Multimode vibration generation system

Figure 6 demonstrates the process of calculating the vibration parameters and cutting velocity for generating the multimode vibration based on the targeted surface profile. In this example, a trapezoidal wave with a wavelength of λ_1 and an amplitude of 0.7 $\mu m_{p\text{-}p}$ (see Fig. 6(a)) is selected as the target profile. First, the target profile is spatially Fourier transformed and the result is plotted against the inverse of the wavelength (Fig. 6(b)). The wavelengths, λ_1 and λ_3, and amplitudes, A_1 and A_3, are obtained. λ_3^{-1} is three times λ_1^{-1}, and A_1 is the amplitude of the first mode (f_1) and A_3 is the amplitude of the third mode (f_3). Note that there are quintuple and higher integer-multiple components, but these higher-order components are neglected here. The first and third mode vibrations are determined, and the sum of these two modes becomes the multimode vibration (Fig. 6(c)). To induce this multimode vibration in the device, the input voltage is calculated by using the measured transfer function of the device. Specifically, the inverse transfer function is utilized (see Fig. 6(d)). In other words, when the necessary displacement of the multimode vibration is expressed as $\mathrm{A} = A_1 \sin(2\pi f_1 t) + A_3 \sin(2\pi f_3 t + \phi)$, the input voltage is obtained as $\mathrm{V} = A_1/G_1 \sin(2\pi f_1 t - \phi_1) + A_3/G_3 \sin(2\pi f_3 t - \phi_3 + \phi)$. The nominal cutting speed V_c is calculated by using

$$V_c = f_1\lambda_1 = f_3\lambda_3. \quad (5)$$

The tool tip trajectory is the summation of the feed motion of the tool in the cutting direction and the induced multimode vibration in the depth-of-cut direction. The tool trajectory is then transferred to the cut surface as the textured profile (Fig. 6(e)). The generated profile is dull compared with the target profile because the quintuple and higher integer-multiple components have been neglected. It is expected that if a vibrator with the fifth mode is considered and designed, the generated profile can be more identical to the target profile.

Based on the proposed system, three types of wave forms, namely trapezoidal, triangular, and distorted triangular waves, are induced and measured without the cutting load on the device. The parameters for the target profiles and input voltages are summarized in Table 1. Figure 7 shows the target profiles, input voltage profiles, and output vibrations. The measurement results of the output vibration (black solid lines) show good agreement with the theoretical vibration profiles (green solid lines). It can be concluded that proper voltage profiles can be identified through the proposed system and that the developed device can generate designed multimode vibrations.

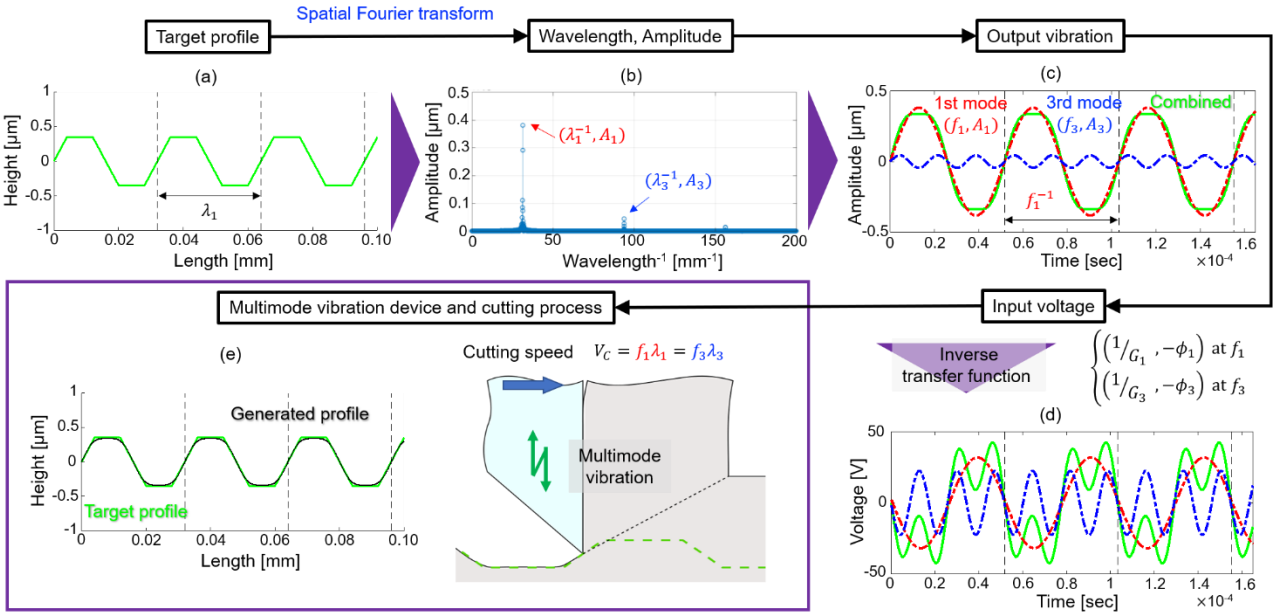

Fig. 6 Proposed multimode vibration generation system.

Table 1. Parameters for multimode vibrations

Type	Target profile			Input voltage			
				1st mode		3rd mode	
	Wavelength λ_1 [mm]	Amplitude [$\mu m_{0\text{-}p}$]	Phase difference ϕ [deg]	Amplitude V_1 [$V_{0\text{-}p}$]	Phase $-\phi_1$	Amplitude V_3 [$V_{0\text{-}p}$]	Phase $-\phi_3+\phi$
Trapezoidal wave	0.032	0.350	0	31.85	-176.22	22.51	-175.96
Triangular wave	0.030	0.547	180	40.92	-176.22	18.37	4.04
Distorted triangular wave	0.028	0.304	180	19.24	-176.22	39.27	4.04

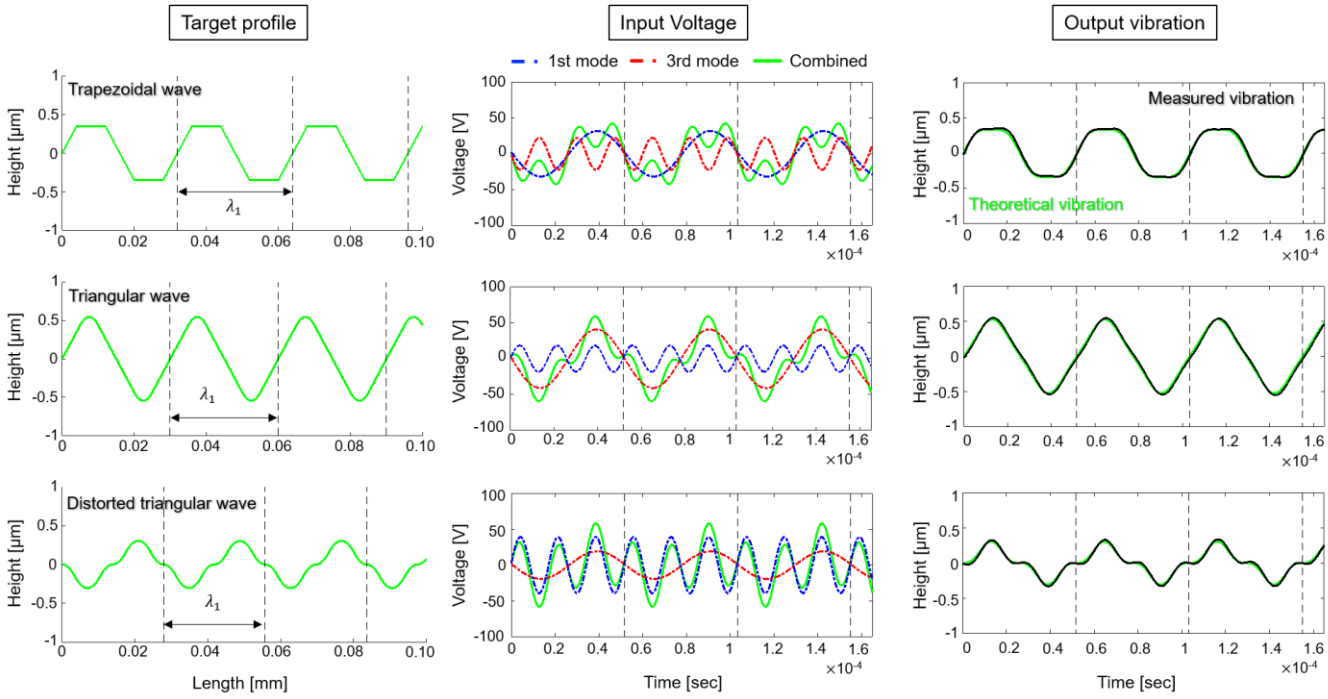

Fig. 7 Measurement results of multimode vibrations.

5. Highly-efficient and highly-flexible surface texturing

In order to verify the applicability of the proposed highly-efficient and highly-flexible surface texturing, cutting experiments are performed on the precision lathe equipped with the developed ultrasonic multimode vibration device. Figure 8 shows a photograph of the experimental setup. Electroless NiP (10 wt% P, average thickness of 30 μm) coated hardened die steel is used as the workpiece. The top surface of the cylindrical workpiece is textured. A single crystalline diamond tool with a nose radius of 1.0 mm is used to obtain optical quality surfaces. The experimental conditions are summarized in Table 2. The cutting conditions, i.e., spindle speed and feed speed, are determined based on the target profiles and cutting ranges (range from minimum to maximum diameter of workpiece). In these texturing experiments, the cutting speed is within the range of 26–39 m/min. This is approximately 30 times faster than the cutting speed of conventional precision surface texturing methods [25]. This increase in the cutting speed results from the direct utilization of ultrasonic vibrations.

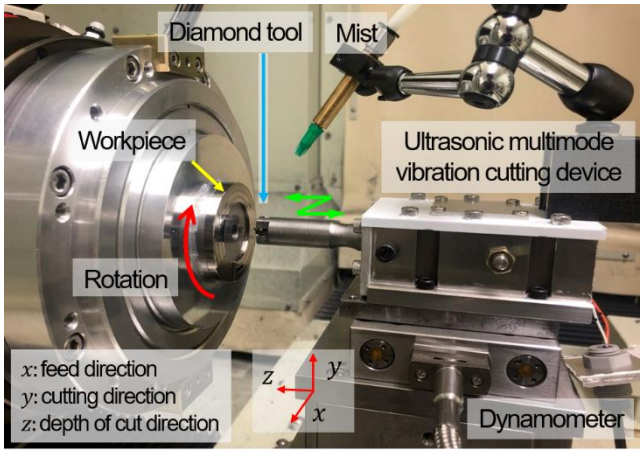

Fig. 8 Experimental setup for highly-efficient and highly-flexible micro/nano surface texturing.

The input voltage profile for the multimode vibrations and the temperature of the temperature-controlled room are identical to those of the measurement setup described in Chapter 4. The nominal depth of cut (see Fig.1) is varied in the range of 0 to 2 μm. During the experiments, the cutting forces are measured using a dynamometer (Kistler, 9256C), and the current and voltage signals are also measured. After the experiments, the surfaces are observed using an optical microscope and the profiles are measured using a 3D optical surface profiler (Zygo, NewView7300). The tool tip is also observed after the experiments by using an optical microscope (Nikon, MM-40/L3U).

Figure 9 shows an example of the measured cutting forces, current signal, and power during one path of the cutting for the triangular wave profile at a nominal depth of cut of approximately 2 μm. The principal and thrust forces reach approximately 0.4 and 0.2 N, respectively. The current is close to zero because the input frequencies are close to the anti-resonant frequencies. Moreover, since the quality factor of the developed system is designed high, i.e. the damping and energy loss is low, the power is close to zero at those anti-resonant modes. It can also be observed that the current and power do not change during cutting. In addition, they are close to those before/after cutting (air-cutting). The raw data were processed by a low-pass filter with a cutoff frequency of 1000 Hz to check the change in the vibration states which might be caused by the cutting load. The filtered data (red dashed lines in Fig. 9) do not change either before/during/after cutting. It can thus be concluded that the amount of load in these experiments does not affect the vibration states of the device. It can also be expected that the induced multimode vibration is constant during the cutting. This will be confirmed by the comparison between the cut surface profiles and the theoretical profiles.

Table 2. Experimental conditions for highly-efficient and highly-flexible surface texturing

Workpiece					
Material	Electroless NiP coating (10 wt% P)				
Diameter	Φ30.2 - Φ50 [mm]				
Hardness	HV 500				
Tool					
Material	Single Crystalline Diamond				
Nose radius	1 mm				
Rake / Clearance angle	0 / 10 °				
Cutting conditions					
Type	Spindle speed [rpm]	Feed speed [mm/min]	Cutting range [mm]	Cutting speed [m/min]	Nominal depth of cut
Trapezoidal	223	22.59	Φ43.4 - Φ50	30.3 - 35.0	0 - 2 μm
Triangular	277	30.80	Φ36.8 - Φ43.4	26.2 - 31.0	
Distorted triangular	337	34.87	Φ30.2 - Φ36.8	32.0 - 39.0	

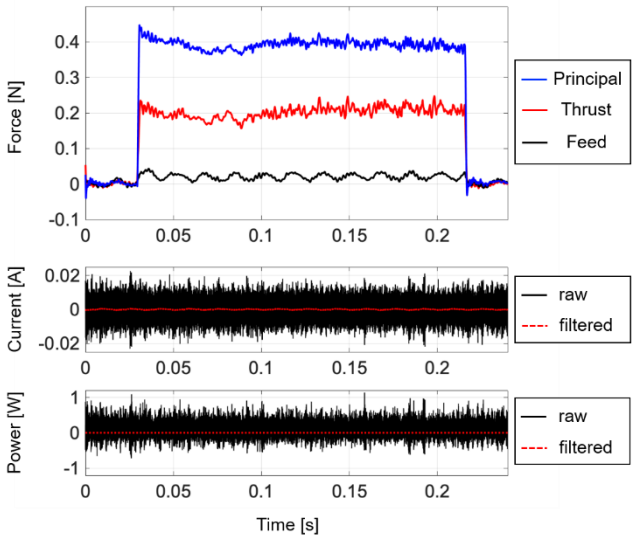

Fig. 9 Measured forces, current, and power. (Target profile: triangular wave, nominal depth of cut: 2 μm)

Figure 10 shows the textured surfaces of the trapezoidal, triangular, and distorted triangular waves. These results show that optical-quality surfaces without undesirable vibration marks or defects can be obtained by using the proposed cutting method. Figure 11 shows the measured profiles when the nominal depth of cut is approximately 2 μm. Compared to the theoretical profiles (black solid lines in Fig. 11), the textured profiles (red dashed lines in Fig. 11) show good agreement without a decrease or increase in the magnitude. Figure 12 shows a microphotograph of the rake and flank faces of the tool after the experiments.

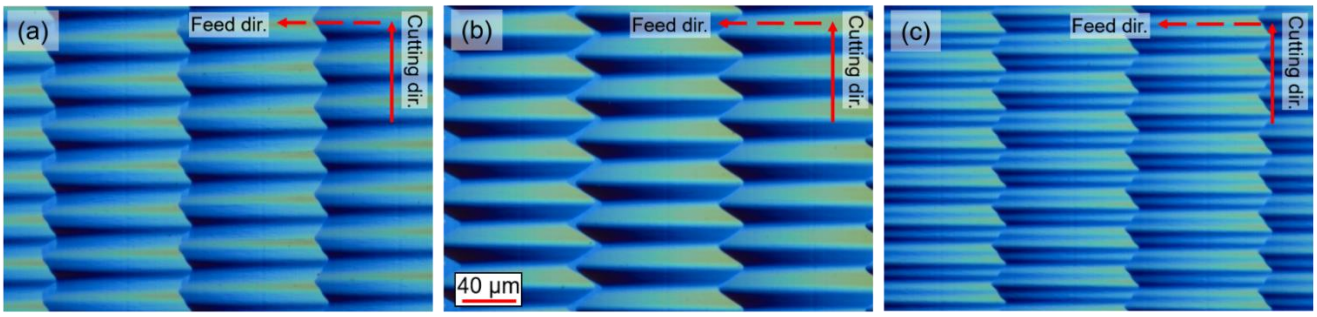

Fig. 10 Optical microphotographs of textured surfaces: (a) trapezoidal, (b) triangular, and (c) distorted triangular waves.

It can be seen that the proposed cutting process does not cause any tool damage or microchipping. This is because the relationship between the clearance angle and the maximum slope of the profiles are considered when the target profiles were designed to ensure that the maximum slopes of the profiles do not exceed the clearance angle.

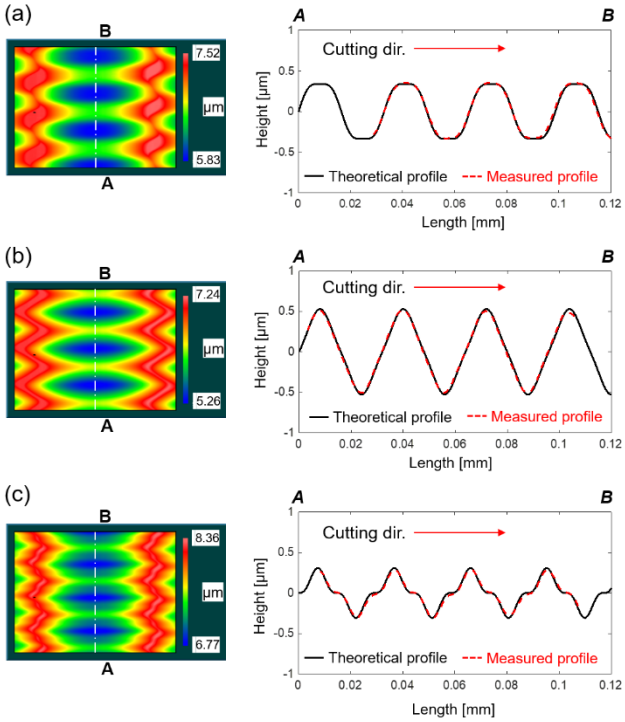

Fig. 11 Surface profiles of textured surfaces: (a) trapezoidal, (b) triangular, and (c) distorted triangular waves.

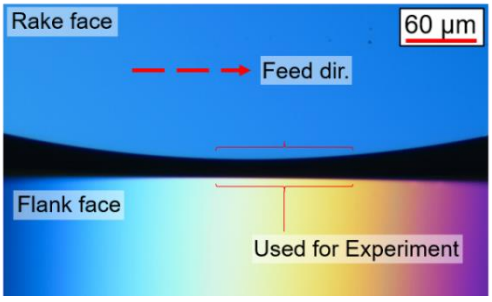

Fig. 12 Microphotograph of cutting edge after surface texturing.

The above textured surfaces are the examples where the whole parts of multimode vibrations are transferred to the cut surfaces. On the other hand, it is also possible to transfer only a part of the multimode vibration by adjusting the depth of cut. Figure 13 shows an example where the nominal depth of cut is the same as the amplitude of the distorted triangular wave. With this multimode vibration cutting, round-edged dimples can be machined on the surface. Note that this kind of highly-flexible texturing is impossible with the conventional resonant vibration cutting devices because those devices can only induce the sinusoidal or distorted sine wave vibration profiles.

Based on the above experimental results, it can be concluded that the proposed cutting device is effective for highly-efficient and highly-flexible surface texturing because of its high nominal cutting speed and ability to generate various wave forms.

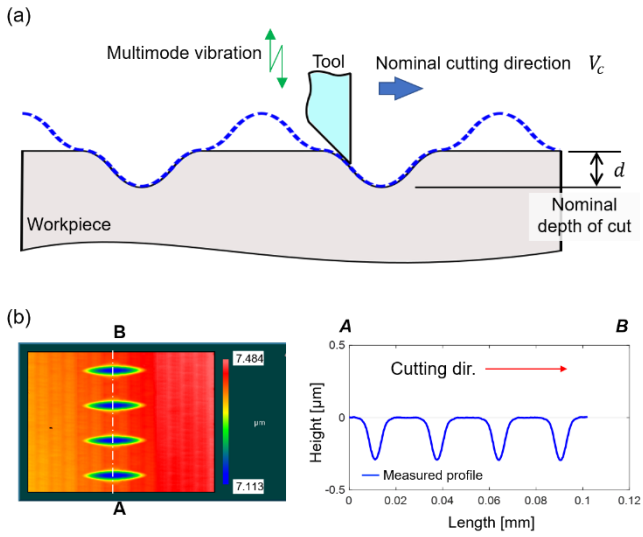

Fig. 13 Round-edged dimple machining with multimode vibration cutting: (a) cutting process with distorted triangular wave, (b) measurement results of textured surface.

6. Conclusions

"Multimode Vibration Cutting" was proposed for highly-efficient and highly-flexible surface texturing. The newly developed multimode vibration generation system and ultrasonic multimode vibration cutting device were demonstrated. In this study, the first and third resonant modes in the depth-of-cut direction were utilized for ultrasonic multimode vibration. By combining the vibrations by those modes, it is possible to generate various shapes of vibrations at ultrasonic frequencies. Since high-resonant frequencies are used directly to machine the surface textures, a high nominal cutting speed can be applied; high

efficiency can be achieved. Cutting experiments were also performed with the developed cutting tool. Three different target profiles were textured on a Ni–P coated plate at a high cutting speed of approximately 32.5 m/min. After the experiments, the textured profiles were compared with the theoretical profiles, and it was observed that the profiles show good agreement. It can be concluded that the proposed ultrasonic multimode vibration cutting method is the only method which realizes highly-efficient and highly-flexible micro/nano surface texturing.

Funding sources

This study was supported partially by the Priority Research and Development of "Next-Generation Ultraprecision/Micro Machining of Difficult-to-Cut Mold Materials" from the Osawa Scientific Studies Grants Foundation, and the Program for Building Regional Innovation Ecosystem "Aichi Innovation Ecosystem Project for Next-Generation Automobile" from the Ministry of Education, Culture, Sports, Science and Technology of Japan.

Declaration of competing interests

The authors declare that they have no known competing financial interests or personal relationships that could have appeared to influence the work reported in this paper.

References

[1] Chu, W.S., Kim, C. S., Lee, H.T., Choi, J.O., Park, J.I., Song, J.H., Jang, K.H., Ahn, S.H., "Hybrid Manufacturing in Micro/Nano Scale: A Review", Int. J. Precis. Eng. Manuf.-Green Tech., Vol. 1, No. 1, pp. 75-92, 2014.

[2] Callies, M., Chen, Y., Marty, F., Pepin, A., Quere, D., "Microfabricated textured surfaces for super-hydrophobicity investigations", Microelectronic Engineering, Vol. 78-79, pp. 100-105, 2005.

[3] Sun, L., Jin, S., Cen, S., "Free-form microlens for illumination applications", Applied Optics, Vol. 48, No. 29, pp. 5520-5527, 2009.

[4] Pettersson, U., Jacobson, S., "Influence of surface texture on boundary lubricated sliding contacts", Tribology International, Vol. 36, pp. 857-864, 2003.

[5] Wei, Y.W., Kim, M.R., Lee, D.W., Park, C., Park, S.S., "Effects of Micro Textured Sapphire Tool Regarding Cutting Forces in Turning Operations", Int. J. Precis. Eng. Manuf.-Green Tech., Vol. 4, No. 2, pp. 141-147, 2017.

[6] Kovalchenko, A., Ajayi, O., Erdemir, A., Fenske, G., Etsio, I., "The effect of laser surface texturing on transitions in lubrication regimes during unidirectional sliding contact", Tribology International, Vol 38, pp. 219-225, 2005.

[7] Braun, D., Greiner, C., Schneider, J., Gumbsch, P., "Efficiency of laser surface texturing in the reduction on friction under mixed lubrication", Tribology International, Vol. 77, pp. 142-147, 2014.

[8] Setzu, S., Ferrand, P., Lernodel, G., Romenstain, R., "Photo-lithograpy for 2D optical microstructures in porous silicon: application to nucleation of macropores", Applied Surface Science, Vol. 186, pp. 588-593, 2002.

[9] Qian, S., Zhu, D., Qu, N., Li, H., Yan, D., "Generating micro-dimples array on the hard chrome-coated surface by modified through mask electrochemical micromachining", Int. J. Adv. Manuf. Technol., Vol. 47, pp.1121-1127, 2010.

[10] Evans, C.J., Bryan, J.B., " 'Structured', 'Textured' or 'Engineered' Surfaces", Annals of the CIRP, Vol. 48, No.2, pp. 541-556, 1999.

[11] Zhang, J., Suzuki, N., Shamoto, E., "Advanced Applications of Elliptical Vibration Cutting in Micro/Nanomachining of Difficult-to-Cut Materials", In: Zhang, J., Guo, B., Zhang J., (eds) "Simulation and Experiments of Material-Oriented Ultra-Precision Machining", Springer Tracts in Mechanical Engineering, Springer, pp. 167-200, 2019.

[12] Sun, J., Luo, X., Chang, W., Ritchie, J.M., Chien, J., Lee, A., "Fabrication of periodic nanostructures by single-point diamond turning with focused ion beam built tool tips", Journal of Micromechanics and Microengineering, Vol. 22, No.11, 115014, 2012.

[13] Dow, T.A., Miller, M.H., Falter, P.J., "Application of a fast tool servo for diamond turning of nonrotationally symmetric surfaces", Precision Engineering, Vol. 13, No. 4, pp. 243-250, 1991.

[14] Gao, W., Araki, T., Kiyono, S., Okazaki, Y., Yamanaka, M., "Precision nano-fabrication and evaluation of a large area sinusoidal grid surface for a surface encoder", Precision Engineering, Vol. 27, No. 3, pp. 289-298, 2003.

[15] Suzuki, N., Yokoi, H., Shamoto, E., "Micro/nano sculpturing of hardened steel by controlling vibration amplitude in elliptical vibration cutting", Precision Engineering, Vol. 35, pp. 44-50, 2011.

[16] Zhang, J., Zhang, J., Rosenkranz, A., Suzuki, N., Shamoto, E., "Frictional properties of surface textures fabricated on hardened steel by elliptical vibration diamond cutting", Precision Engineering, Vol. 59, pp. 66-72, 2019.

[17] Zhang, J., Suzuki, N., Wang, Y., Shamoto, E., "Fundamental investigation of ultra-precision ductile machining of tungsten carbide by applying elliptical vibration cutting with single crystal diamond", Journal of Materials Processing Technology, Vol. 214, pp. 2644-2659, 2014.

[18] Lu, X.D., Trumper, D.L., "Ultrafast Tool Servos for Diamond Turning", Annals of the CIRP, Vol. 54, No.1, pp. 383-388, 2005.

[19] Kumabe, J., Precision High Speed Vibration Cutting (in Japanese), 58-143901, Japan Patent Office, 6 August 1983.

[20] Guo, P., Ehmann, K. N., "Development of a tertiary motion generator for elliptical vibration texturing", Precision Engineering, Vol. 37, pp. 364-371, 2013.

[21] Xu, S., Shimada, K., Mizutani, M., Kuriyagawa, T., "Fabrication of hybrid micro/nano-textured surfaces using rotary ultrasonic machining with one-point diamond tool", International Journal of Machine Tools and Manufacture, Vol. 86, pp. 12-17, 2014.

[22] Zhang, S. J., To, S., "A theoretical and experimental investigation into multimode tool vibration with surface generation in ultra-precision diamond turning", International Journal of Machine Tools and Manufacture, Vol. 72, pp.32-36, 2013.

[23] Zhou, X., Zuo C., Liu Q., Wang R., Lin J., "Development of a double-frequency elliptical vibration cutting apparatus for freeform surface diamond machining", Int. J. Adv. Manuf. Technol., Vol. 87, pp.2099-2111, 2016.

[24] Yuan, Y., Zhang D., Jing X., Ehmann F. K., "Freeform surface fabrication on hardened steel by double frequency vibration cutting", Journal of Materials Processing Tech., Vol. 275, 116369, 2020.

[25] Zhang, J., Suzuki, N., Wang, Y., Shamoto, E., "Ultra-precision nano-structure fabrication by amplitude control sculpturing method in elliptical vibration cutting", Precision Engineering, Vol. 39, pp. 86-99, 2015.